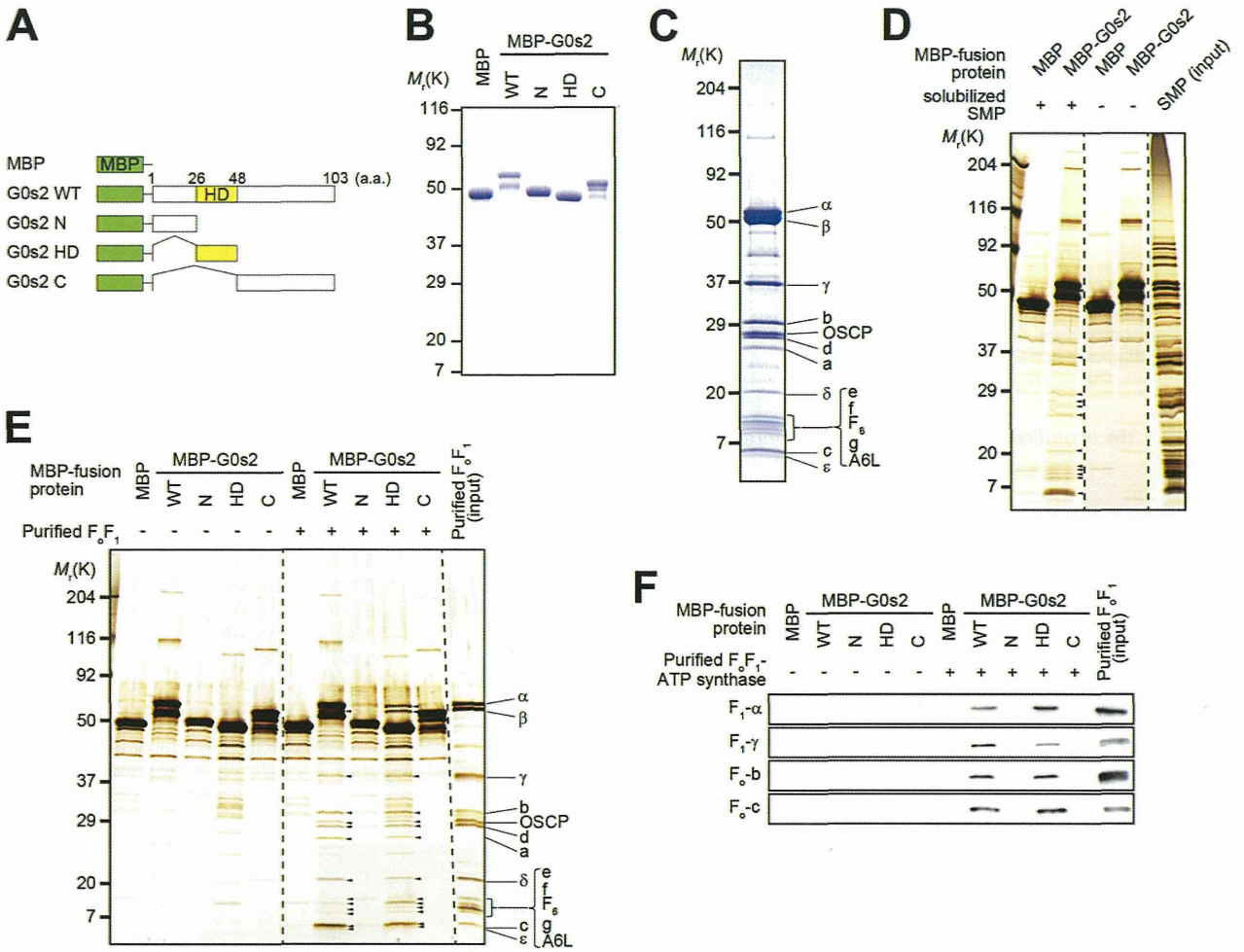

Fig. S5. G0s2 directly interacts with F_oF_1-ATP synthase. (*A*) A schematic representation of recombinant maltose-binding protein (MBP)-fusion proteins purified from *Escherichia coli*. (*B*) Coomassie Brilliant Blue-stained gel of recombinant MBP-fusion proteins purified from *E. coli*. (*C*) Coomassie Brilliant Blue-stained gel of purified F_oF_1-ATP synthase from bovine heart mitochondria. OSCP, oligomycin sensitivity conferral protein. (*D* and *E*) A silver-stained gel of an in vitro pull-down assay using (*D*) submitochondrial particles (SMPs) or (*E*) purified F_oF_1-ATP synthase from bovine heart mitochondria. Arrowheads indicate the F_oF_1-ATP synthase subunits bound to G0s2 protein. (*F*) Immunoblotting of an in vitro pull-down assay using purified F_oF_1-ATP synthase.

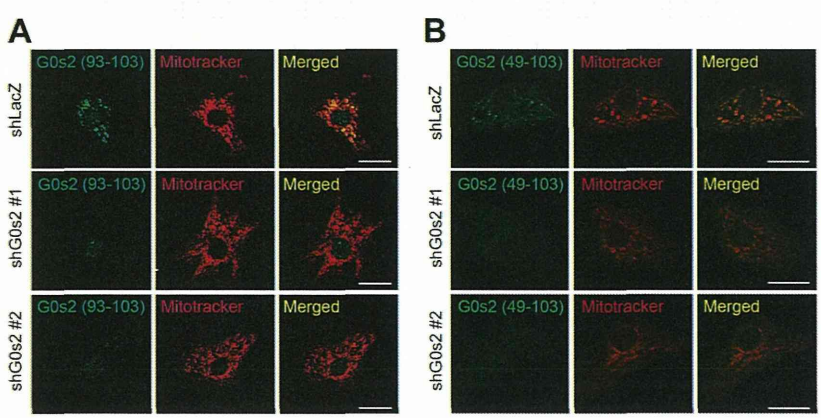

Fig. S6. G0s2 is localized to mitochondria. Immunostaining with an antibody against mouse (*A*) G0s2 (93–103 aa) or (*B*) G0s2 (49–103 aa) in cardiomyocytes expressing shLacZ, shG0s2 #1, and shG0s2 #2. (Scale bars: 20 μm.)

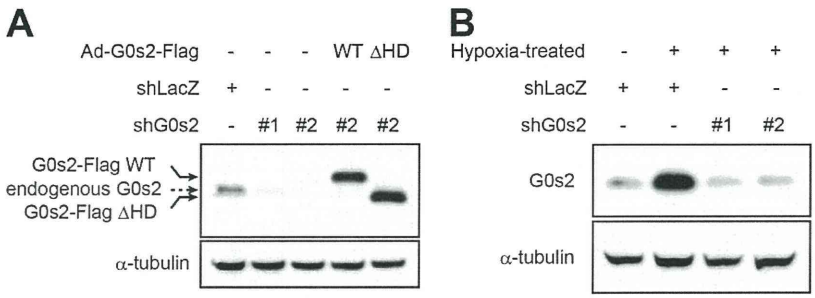

Fig. S7. (*A*) Immunoblotting of G0s2-depleted cardiomyocytes rescued by overexpression of G0s2-Flag. (*B*) Immunoblotting of G0s2-depleted cardiomyocytes under hypoxic conditions. Cardiomyocytes expressing the indicated adenovirus were exposed to hypoxia (1% O_2) for 4 h. The cell lysates were subjected to immunoblotting with anti-G0s2 or α-tubulin antibodies.

Table S1. The identification of proteins that specifically bound to G0s2 by MS

SwissProt accession	Description	Molecular mass (Da)	PLGS score	Peptides	Coverage (%)
ATPA_RAT	ATP synthase subunit-α mitochondrial	59,716	10.5798	10	18.9873
ATPB_RAT	ATP synthase subunit-β mitochondrial	56,318	10.5798	11	24.1966
ATPG_RAT	ATP synthase γ-chain	32,975	10.523	2	7.3826
ATP5F1_RAT	ATP synthase subunit b mitochondrial	28,850	10.5796	2	3.9063
ATPO_RAT	ATP synthase subunit O mitochondrial	23,382	10.5796	5	23.9437
ATP5H_RAT	ATP synthase subunit d mitochondrial	18,751	10.5796	2	13.0435
ATPD_RAT	ATP synthase subunit-δ mitochondrial	17,584	10.5796	2	13.6905
D3ZAF6_RAT	ATP synthase H transporting mitochondrial Fo complex subunit f isoform 2	10,972	10.5796	2	22.3404

A PLGS score was calculated by the Protein Lynx Global Server (PLGS; PLGS 2.4) software using a Monte Carlo algorithm to analyze all of the available MS data; this score is a statistical measure of the accuracy of assignation. A higher score implies a greater confidence in the identity of the protein.

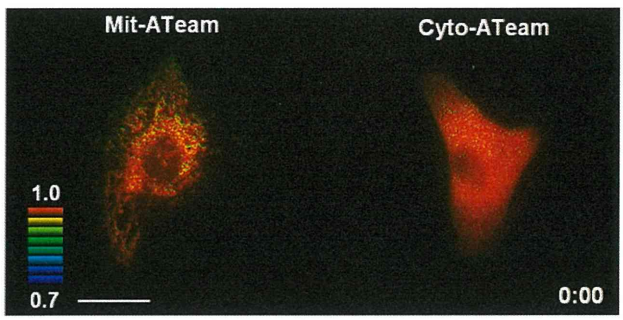

Movie S1. Time-lapse imaging of the (*Left*) Mit-ATeam and (*Right*) Cyto-ATeam fluorescence in cardiomyocytes before and after the addition of oxidative phosphorylation inhibitor. YFP/CFP ratiometric pseudocolored images were obtained every 1 min for 25 min. Oligomycin A (0.01 μg/mL), an inhibitor of F_oF_1-ATP synthase, was added at time point 5 min. (Scale bar: 20 μm.)

Movie S1

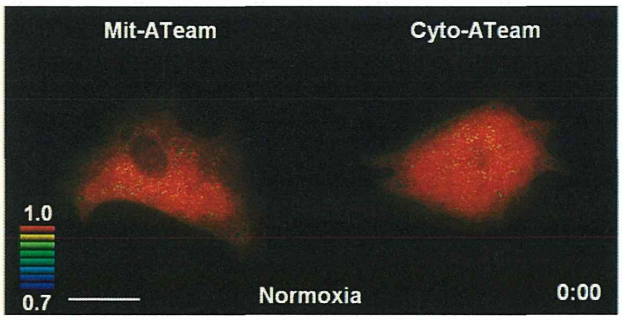

Movie S2. Time-lapse imaging of the (*Left*) Mit-ATeam and (*Right*) Cyto-ATeam fluorescence in cardiomyocytes exposed to hypoxia. YFP/CFP ratiometric pseudocolored images were obtained every 30 min for 3 h. Cells are exposed to 1% hypoxia from the time point 30 min. (Scale bar: 20 μm.)

Movie S2

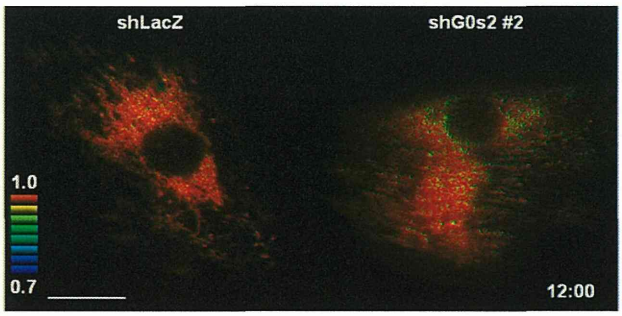

Movie S3. Time-lapse imaging of the Mit-ATeam fluorescence in cardiomyocytes that expressed (*Left*) shLacZ or (*Right*) shG0s2 #2. YFP/CFP ratiometric pseudocolored images were obtained every 1 h for 12 h. An inhibitor of F_oF_1-ATP synthase (1 μg/mL oligomycin A) was added at the end of time-lapse imaging to completely inhibit ATP synthesis. (Scale bar: 20 μm.) The indicated times designate the periods after adenovirus infection.

Movie S3

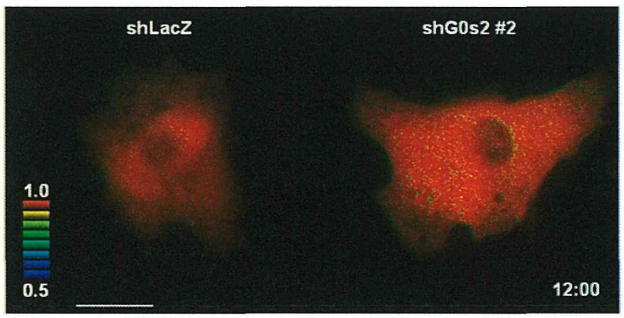

Movie S4. Time-lapse imaging of the Cyto-ATeam fluorescence in cardiomyocytes that expressed (*Left*) shLacZ or (*Right*) shG0s2 #2. YFP/CFP ratiometric pseudocolored images were obtained every 1 h for 12 h. Inhibitors of both glycolysis (10 mM 2-deoxyglucose) and F_oF_1-ATP synthase (1 μg/mL oligomycin A) were added at the end of the time-lapse imaging to decrease the cytosolic ATP concentration. (Scale bar: 20 μm.) The indicated times designate the periods after adenovirus infection.

Movie S4

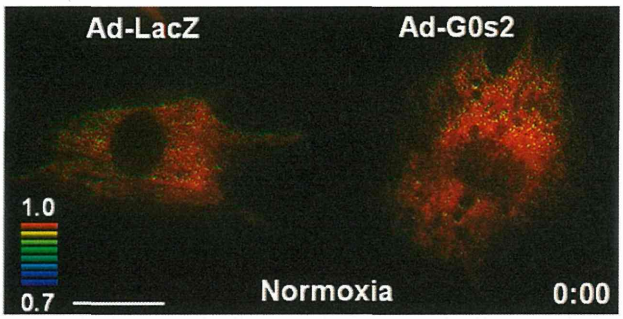

Movie S5. Time-lapse imaging of the Mit-ATeam fluorescence in cardiomyocytes that expressed (*Left*) LacZ or (*Right*) G0s2 during hypoxia and reoxygenation. YFP/CFP ratiometric pseudocolored images were obtained every 30 min for 4 h. The cells were exposed and imaged under hypoxic condition from the time point 30 min to 4 h. (Scale bar: 20 μm.)

Movie S5

OPEN ACCESS Freely available online

PLoS one

A Crucial Role of Activin A-Mediated Growth Hormone Suppression in Mouse and Human Heart Failure

Noritoshi Fukushima[1,2☯], Katsuhisa Matsuura[1,3*☯], Hiroshi Akazawa[4☯], Atsushi Honda[1], Toshio Nagai[5], Toshinao Takahashi[5], Akiko Seki[1], Kagari M. Murasaki[1], Tatsuya Shimizu[3], Teruo Okano[3], Nobuhisa Hagiwara[1,2], Issei Komuro[4*]

1 Department of Cardiology, Tokyo Women's Medical University, Tokyo, Japan, **2** Global Centers of Excellence (GCOE) Program, Tokyo Women's Medical University, Tokyo, Japan, **3** Institute of Advanced Biomedical Engineering and Science, Tokyo Women's Medical University, Tokyo, Japan, **4** Department of Cardiovascular Medicine, Osaka University Graduate School of Medicine, Osaka, Japan, **5** Department of Cardiovascular Science and Medicine, Chiba University Graduate School of Medicine, Chiba, Japan

Abstract

Infusion of bone marrow-derived mononuclear cells (BMMNC) has been reported to ameliorate cardiac dysfunction after acute myocardial infarction. In this study, we investigated whether infusion of BMMNC is also effective for non-ischemic heart failure model mice and the underlying mechanisms. Intravenous infusion of BMMNC showed transient cardioprotective effects on animal models with dilated cardiomyopathy (DCM) without their engraftment in heart, suggesting that BMMNC infusion improves cardiac function *via* humoral factors rather than their differentiation into cardiomyocytes. Using conditioned media from sorted BMMNC, we found that the cardioprotective effects were mediated by growth hormone (GH) secreted from myeloid (Gr-1(+)) cells and the effects was partially mediated by signal transducer and activator of transcription 3 in cardiomyocytes. On the other hand, the GH expression in Gr-1(+) cells was significantly downregulated in DCM mice compared with that in healthy control, suggesting that the environmental cue in heart failure might suppress the Gr-1(+) cells function. Activin A was upregulated in the serum of DCM models and induced downregulation of GH levels in Gr-1(+) cells and serum. Furthermore, humoral factors upregulated in heart failure including angiotensin II upregulated activin A in peripheral blood mononuclear cells (PBMNC) via activation of NFκB. Similarly, serum activin A levels were also significantly higher in DCM patients with heart failure than in healthy subjects and the GH levels in conditioned medium from PBMNC of DCM patients were lower than that in healthy subjects. Inhibition of activin A increased serum GH levels and improved cardiac function of DCM model mice. These results suggest that activin A causes heart failure by suppressing GH activity and that inhibition of activin A might become a novel strategy for the treatment of heart failure.

Citation: Fukushima N, Matsuura K, Akazawa H, Honda A, Nagai T, et al. (2011) A Crucial Role of Activin A-Mediated Growth Hormone Suppression in Mouse and Human Heart Failure. PLoS ONE 6(12): e27901. doi:10.1371/journal.pone.0027901

Editor: Piero Anversa, Brigham and Women's Hospital, United States of America

Received August 21, 2011; **Accepted** October 27, 2011; **Published** December 28, 2011

Funding: This study was supported by: The Global Centers of Excellence (COE) Program, Multidisciplinary Education and Research Center for Regenerative Medicine (MERCREM), from the Japanese Ministry of Education, Culture, Sports, Science and Technology (to N. Fukushima); a Grant-in-Aid for Scientific Research, Developmental Scientific Research, and Scientific Research from the Japanese Ministry of Education, Culture, Sports, Science and Technology; Uehara Memorial Research Grant (to KM); Grants from the Japanese Ministry of Education, Culture, Sports, Science and Culture and Health and Labor Sciences Research Grants (to HA); and a Grant-in-Aid for Scientific Research on Priority Areas and for Exploratory Research from the Japanese Ministry of Education, Culture, Sports, Science and Technology (to IK). The funders had no role in study design, data collection and analysis, decision to publish, or preparation of the manuscript.

Competing Interests: The authors have declared that no competing interests exist.

* E-mail: kmatsuura@abmes.twmu.ac.jp (KM); komuro-tky@umin.ac.jp (IK)

☯ These authors contributed equally to this work.

Introduction

Heart failure is a major cause of mortality in many countries. Infusion of bone marrow-derived mononuclear cells (BMMNC) is expected as a novel treatment of heart failure. Animal experiments and clinical trials have shown that BMMNC infusion ameliorates cardiac dysfunction after acute myocardial infarction and chronic myocardial ischemia [1]–[4]. Although the outcomes vary among trials, recent meta-analyses revealed that cardiac function slightly improves following BMMNC infusion for ischemic heart diseases [5], [6]. Bone marrow cells were reported to be incorporated into the damaged myocardium and to differentiate into various cell types including cardiomyocytes [7]. However, whether bone marrow-derived stem cells can differentiate into many cardiomyocytes is still an open question [8]. There are many reports indicating that transplantation of various types of stem cells improves the cardiac function of ischemic hearts, mainly by paracrine factors which induce angiogenesis and cardioprotection [9]–[11]. Since the effects of BMMNC infusion for non-ischemic cardiomyopathy remain unknown, we examined whether BMMNC infusion also improves cardiac function of non-ischemic cardiomyopathy.

Results

Preparation of non-ischemic dilated cardiomyopathy (DCM) mice

Two kinds of non-ischemic DCM mice were used. The first model was generated by transgenic overexpression of a mutant epidermal growth factor receptor (EGFR) with C-terminal truncation (EGFRdn). The expression of mutant EGFRdn is

activated by the cardiomyocyte-specific α-myosin heavy chain (αMHC) promoter (Figure 1A, Figure S1). EGFRdn mice exhibited heart failure and died at 5–30 weeks of age (Figure 1B). Gross inspection of the EGFRdn hearts showed global chamber dilatation with marked wall thinning (Figure 1C). The heart/body weight ratio was approximately 1.5-fold higher at 6 weeks of age in EGFRdn mice than in wild-type mice (Figure 1D). Echocardiography showed a significant decrease in the fractional shortening (FS) together with chamber dilatation (Figure 1E). In the second model, cardiomyopathy was induced by intraperitoneal injection of doxorubicin in wild-type mice. Doxorubicin-induced cardiomyopathy (DOX) mice showed marked dilatations of the left ventricular diastolic and systolic dimensions, and reduction of cardiac function (Figure S2).

Intravenous infusion of BMMNC transiently improved the cardiac function in DCM mice

BMMNC (2.0×10^7 cells) were isolated from wild-type healthy mice and intravenously infused *via* the tail veins to 8-week-old EGFRdn mice and 11-week-old DOX mice. An equal volume of PBS was infused into control mice. Three days after infusion, echocardiography showed that the FS was significantly improved in BMMNC-treated EGFRdn (Figure 2A) and DOX (Figure 2A) mice, compared with the respective controls. However, these effects were lost by 14 d after infusion (Figure 2A). When the infusion was repeated every 2 weeks, cardiac function showed improvements for >50 d (Figure 2B).

Although infusion of BMMNC is not promising for the treatment of heart failure, we may be able to apply alternative treatment if we understand the underlying mechanisms of beneficial effects of BMNNC infusion. To elucidate the mechanisms, we infused BMMNC derived from GFP mice. Although many GFP-positive cells were observed in the peripheral blood and the spleen at 3 d after infusion (Figure 2C, D), none were found in the heart, lung, liver, kidney or skeletal muscle (Figure 2E). At day 14, few GFP-positive cells were observed even in the peripheral blood (Figure 2C). This was consistent with the observation that BMMNC infusion improved cardiac function at day 3, but not at day 14. These results suggest that BMMNC infusion improves the systolic function of DCM mice not by transdifferentiation of BMMNC into cardiomyocytes but probably by humoral factors secreted from BMMNC. Size of each cardiomyocyte was larger in BMMNC-infused EGFRdn mice than in PBS-infused EGFRdn mice when infusions were repeated every 2 weeks for 8 weeks (i.e.,

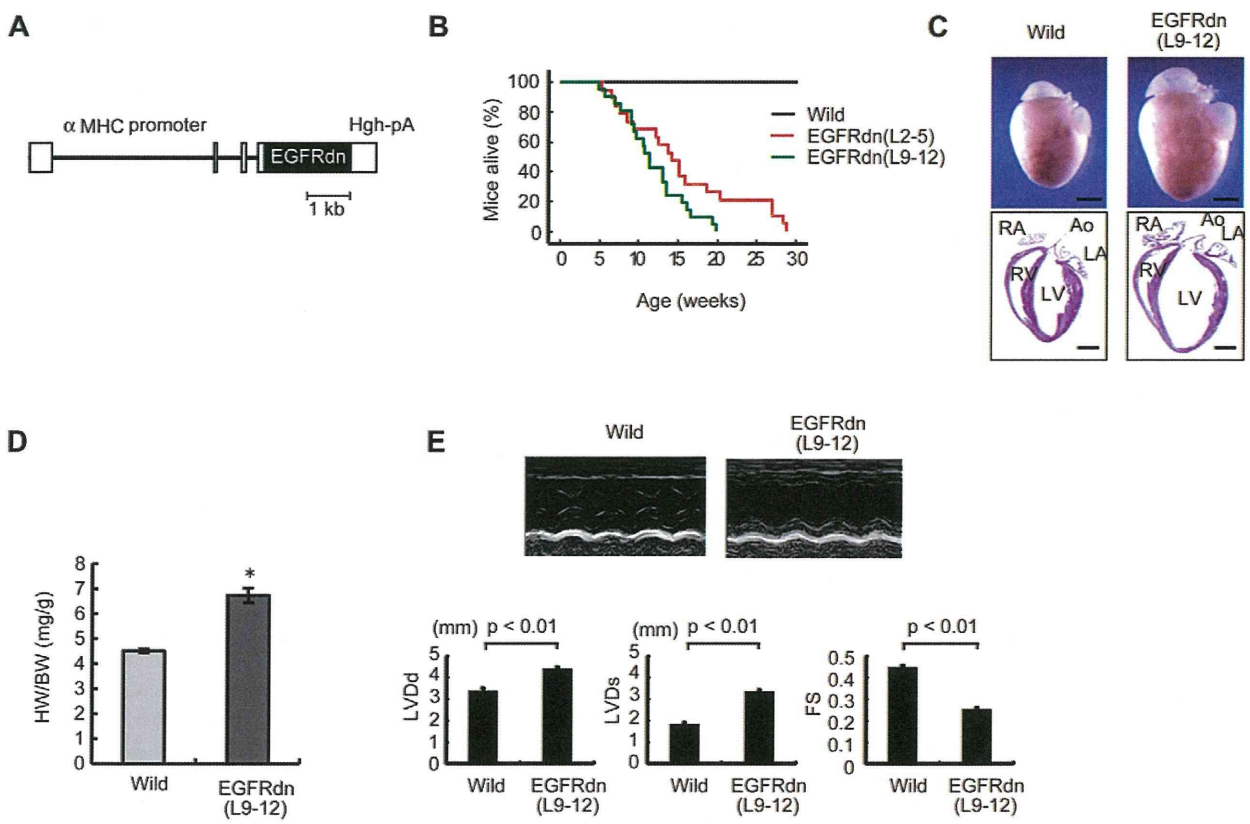

Figure 1. Transgenic overexpression of EGFRdn in the heart causes progressive heart failure. (A) Schematic representation of the cDNA construct used to generate EGFRdn mice. The construct contains an αMHC promoter, human EGFRdn cDNA and a human *growth hormone* polyadenylation signal (Hgh-pA). (B) Kaplan-Meier survival curves for wild-type ($n=62$) and EGFRdn (L2–5, $n=19$; L9–12, $n=21$) mice, showing a significant reduction in the survival rates in EGFRdn mice (log rank test, $P<0.0001$). (C) Gross morphology of whole hearts (upper panels) and longitudinal sections (lower panels) of hearts from wild-type and EGFRdn mice (L9–12) at 6 weeks of age. Ao, aorta; LA, left atrium; LV, left ventricle; RA, right atrium; RV, right ventricle. Scale bars: 2 mm. (D) Heart-to-body weight ratios (HW/BW) of wild-type ($n=9$) and EGFRdn (L9–12, $n=7$) mice at 6 weeks of age. *$P<0.01$. (E) Echocardiographic analysis. The upper photographs show representative M-mode images. The lower graphs show the left ventricular diastolic and systolic dimensions and FS of 8 week-old EGFRdn mice (L9–12) ($n=23$) and age-matched wild-type mice ($n=10$). LVDd, left ventricular diastolic dimension; LVDs, left ventricular systolic dimension. Data are means ± s.e.m.
doi:10.1371/journal.pone.0027901.g001

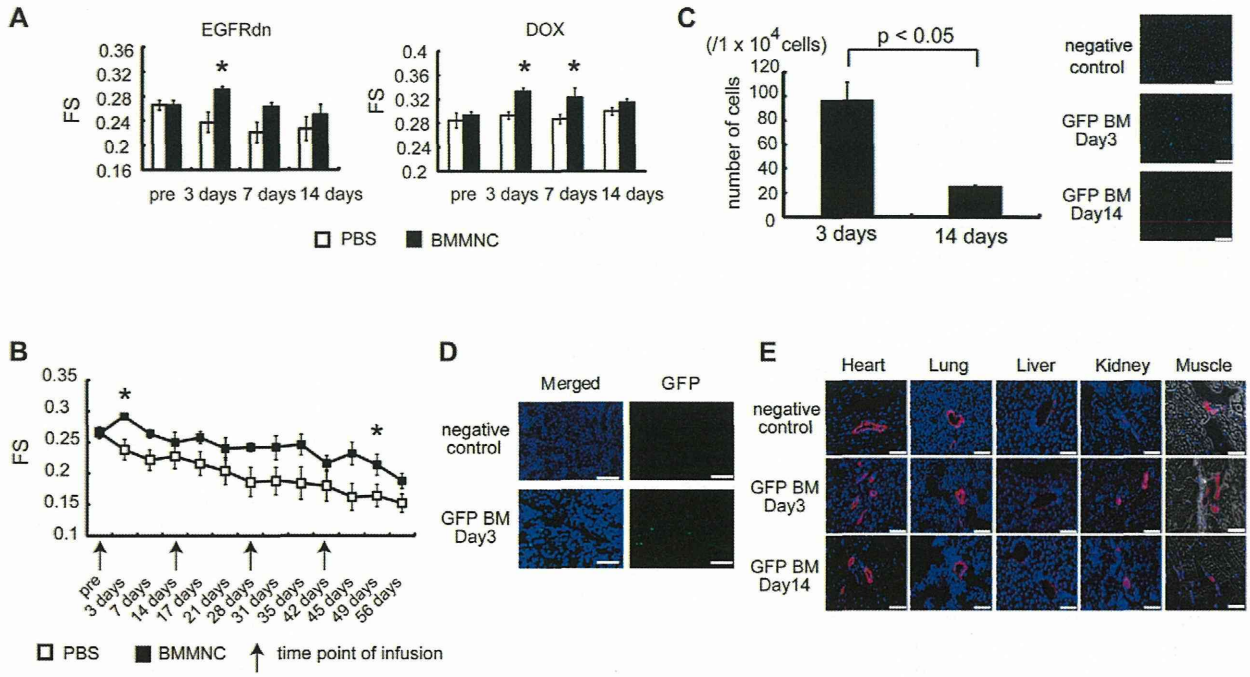

Figure 2. BMMNC infusion transiently improved the cardiac function of DCM mice. (A) Echocardiographic analysis. Transient improvements of FS were observed at 3 d in the BMMNC-treated group, but not the control (PBS) group, in EGFRdn mice (left), and at 3 and 7 d in DOX-treated mice (right). *$p<0.05$ versus PBS ($n=8$ per group). (B) Repeated-infusion experiments. BMMNC were infused every 2 weeks. A similar pattern of improvement in FS was observed after each infusion. *$p<0.05$ versus PBS ($n=8$ per group). (C–E) Immunohistochemical analysis. (C) Left, the number of GFP-positive BMMNC in peripheral blood ($n=3$). Right, photomicrographs of peripheral blood. Nuclei were stained with Hoechst 33258 (blue). Scale bars, 75 μm. (D) Images of the spleen 3 d after infusion. Many GFP-positive cells were observed in the spleen (lower photographs). Upper photographs, negative control. Nuclei were stained with Hoechst (blue color). Scale bars, 25 μm. (E) No GFP-positive cells were observed in any organs. Upper photographs, negative control. Middle and lower photographs, images taken at 3 and 14 d, respectively, after infusion. The vessels were stained with smooth muscle cell actin (red). Nuclei were stained with Hoechst 33258 (blue). The photographs of muscle are merged fluorescent and phase-contrast images. Scale bars, 75 μm. Data are means ± s.e.m.
doi:10.1371/journal.pone.0027901.g002

4 injections) (Figure S3). There were no changes in capillary density or the number of apoptotic cells in the heart between the BMMNC-infused group and the control group (data not shown).

BMMNC-derived conditioned medium (CM) improved cardiomyocyte contractility

To elucidate whether factors secreted from BMMNC were involved in their beneficial effects on cardiac function, we first examined the effects of CM from BMMNC on the contractility of cultured cardiomyocytes of neonatal rats. After serum starvation for 12 h, cardiomyocytes were challenged with culture medium conditioned by BMMNC. Cell shortening was significantly enhanced and beating rate was markedly increased at 30 min and at 12 h after starting culture with the CM, compared with those in untreated cells (Figure 3A), suggesting that BMMNC secrete factors that positively affect cardiomyocyte contractility. Flow cytometric analysis revealed that BMMNC consisted of several cell populations including myeloid (Gr-1(+) cells, ~40%), erythroid (TER119(+) cells, ~20%), and lymphoid cells (B220(+) cells, ~20%) (Figure S4). The individual cell populations, including the lineage-negative population of cells, were sorted by magnetic beads. The isolated cells were 0.8×10^7 Gr-1(+) cells, 0.4×10^7 B220(+) cells, 0.2×10^7 TER(+) cells, and 0.1×10^7 lineage-negative cells from 2.0×10^7 BMMNC. When CM was collected from each population and added to cardiomyocytes starved for 12 h, only the CM from Gr-1(+) cells significantly enhanced cell shortening and increased the beating rate (Figure 3B), suggesting that Gr-1(+) cells mainly contribute to BMMNC-mediated improvements in cardiomyocyte contractility. CM from Gr-1(+) cells or BMMNC isolated from wild-type mice also induced significant hypertrophy of cardiomyocytes (Figure S5). We next examined the effects of CM from Gr-1(+) cells on DOX mice. At 1 and 3 d after the infusion of CM from Gr-1(+) cells, FS was significantly improved, as with infusion of BMMNC (Figure 3C). Furthermore, +dp/dt, as determined by catheterization of the left ventricle, was also improved at 1 d after the infusion, as compared with the control group (Figure 3D). Collectively, these results indicate that factors secreted from Gr-1(+) cells are responsible for BMMNC-induced improvements in cardiac function in DCM mice.

Analysis of factors secreted from Gr-1(+) cells

The CM from wild-type Gr-1(+) cells significantly enhanced cell shortening and increased the beating rate, while CM from EGFRdn Gr-1(+) cells had marginal effects (Figure 4A). This suggests that the factors that improve cardiomyocyte contractility are more abundant in cells of wild-type mice than cells of EGFRdn mice. We next performed DNA microarray analysis to identify the factors involved in these effects. Twenty three genes showed enhanced expression in Gr-1(+) cells from wild-type mice compared with EGFRdn mice (Table 1). The gene which showed the largest difference between two types of mice was growth

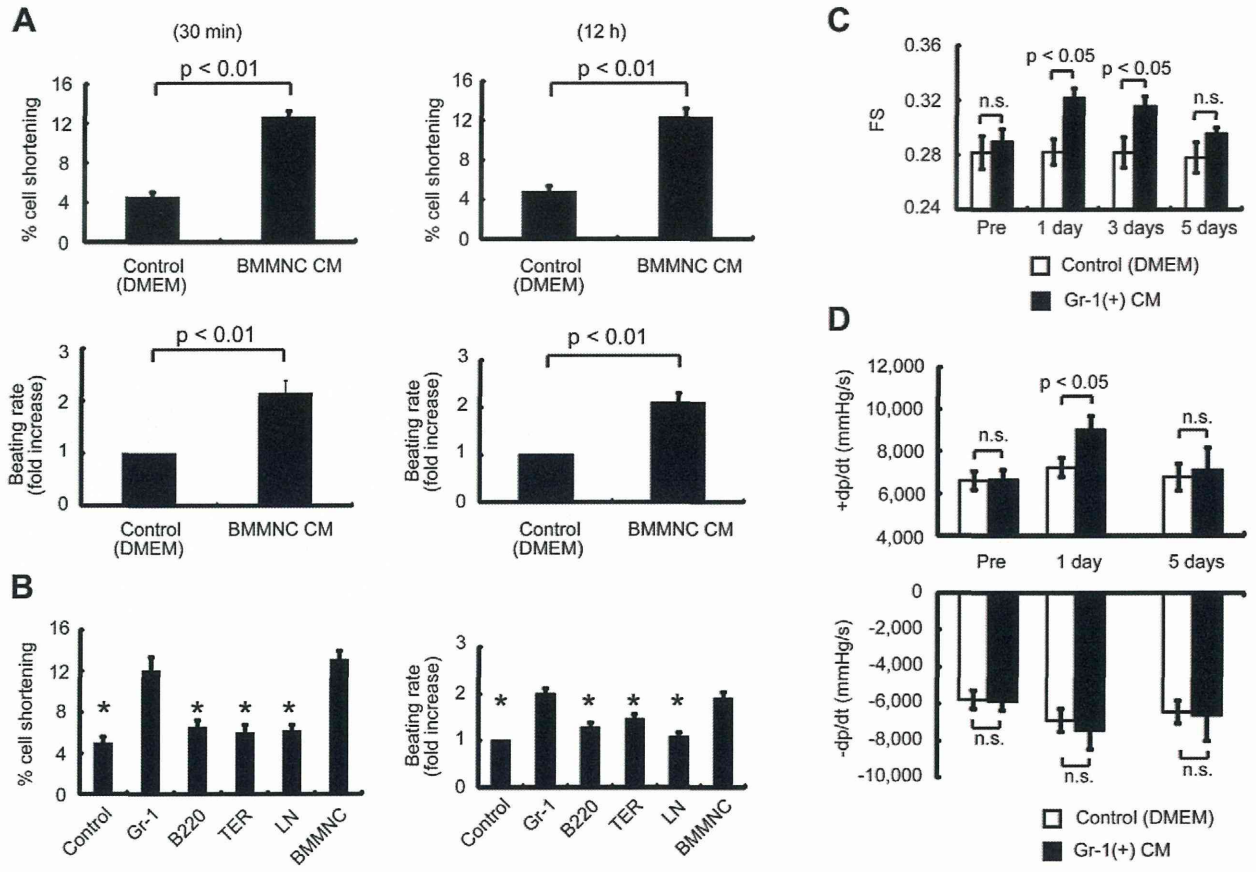

Figure 3. BMMNC-derived CM directly affects cardiomyocyte contractility. (A) Cell shortening and the beating rate of neonatal rat cardiomyocytes were significantly increased after exposure to CM from BMMNC compared with the control ($n = 26$ cells per group). The left and right graphs show the results at 30 min and at 12 h after treatment, respectively. Upper graph, cell shortening. Lower graph, beating rate. (B) CM from Gr-1(+) cells improved the cell shortening and increased the beating rate similar to that achieved by CM from BMMNC ($n = 27$ per group). (C, D) Effects of CM from Gr-1 cells on cardiac function *in vivo*. (C) Echocardiographic analysis ($n = 7$). The infusion of CM from Gr-1(+) cells significantly improved the FS of DOX mice at 1 and 3 d. (D) Infusion of CM from Gr-1(+) cells significantly improved the +dp/dt of DOX mice at 1 d, *in vivo* ($n = 7$). n.s., not significant. Data are means ± s.e.m.
doi:10.1371/journal.pone.0027901.g003

hormone (GH). The reduced expression of GH in Gr-1(+) cells from EGFRdn mice was confirmed by quantitative RT-PCR and ELISA (Figure 4B, C). GH levels were also lower in CM from Gr-1(+) cells isolated from old myocardial infarction (OMI) mice and DOX mice (Figure S6) than in CM from wild-type mice. Consistent with the downregulation of GH secretion from Gr-1(+) cells of heart failure mice, the serum GH levels were also lower in models of heart failure such as DOX, EGFRdn and OMI mice than in wild-type mice (Figure 4E).

Critical role of GH in Gr-1(+) cell-mediated cardioprotection

We examined the role of GH in the effects of Gr-1(+) cell-derived CM using pegvisomant, a specific inhibitor of the GH receptor [12]. Treatment with pegvisomant abolished the enhanced cell shortening and the increased beating rate induced by CM from Gr-1(+) cells (Figure 5A), while the anti-IGF-1 antibody had no effects (Figure 5B). These results suggest that Gr-1(+) cells improved the cardiomyocyte contractility *via* GH, but not *via* IGF-1 *in vitro*. CM from Gr-1(+) cells activated various signaling molecules, including Akt, extracellular signal-regulated kinase (Erk) 1/2, Janus kinase (Jak) 2, signal transducers and activators of transcription (Stat) 3/5 and protein kinase A (PKA) in cardiomyocytes (Figure 5C), and these effects were completely abolished by pegvisomant (Figure 5C). The addition of GH (500 pg/ml), a concentration equivalent to that in the CM from wild-type Gr-1(+) cells, activated the same signaling molecules (Figure 5C), suggesting that CM from Gr-1(+) cells activates Akt, Erk1/2, Jak2, Stat3/5 and PKA through the GH receptor signaling. Furthermore, the CM from Gr-1(+) cells, as well as GH, increased the amount of cyclic AMP (cAMP) in cardiomyocytes, which was also inhibited by pegvisomant (Figure 5D). The improvements in cardiac function induced by CM from Gr-1(+) cells were also abolished by treatment with the GH inhibitor (Figure 5E), whereas the anti-IGF-1 antibody had no effects (Figure 5F). Furthermore, the infusion of CM from Gr-1(+) cells increased the GH levels in serum of DCM mice (Figure 5G). These results suggest that Gr-1(+) cells improve the cardiac contractility *in vivo* also through GH. The BMMNC-mediated improvement in cardiac function of OMI mice was also affected by treatment with pegvisomant (Figure S7), suggesting that GH in BMMNC might have the therapeutic effects on heart failure caused by various etiologies.

Since Stat 3 is one of the important downstream targets of the GH receptor in cardiomyocytes (Figure 5C), we examined the

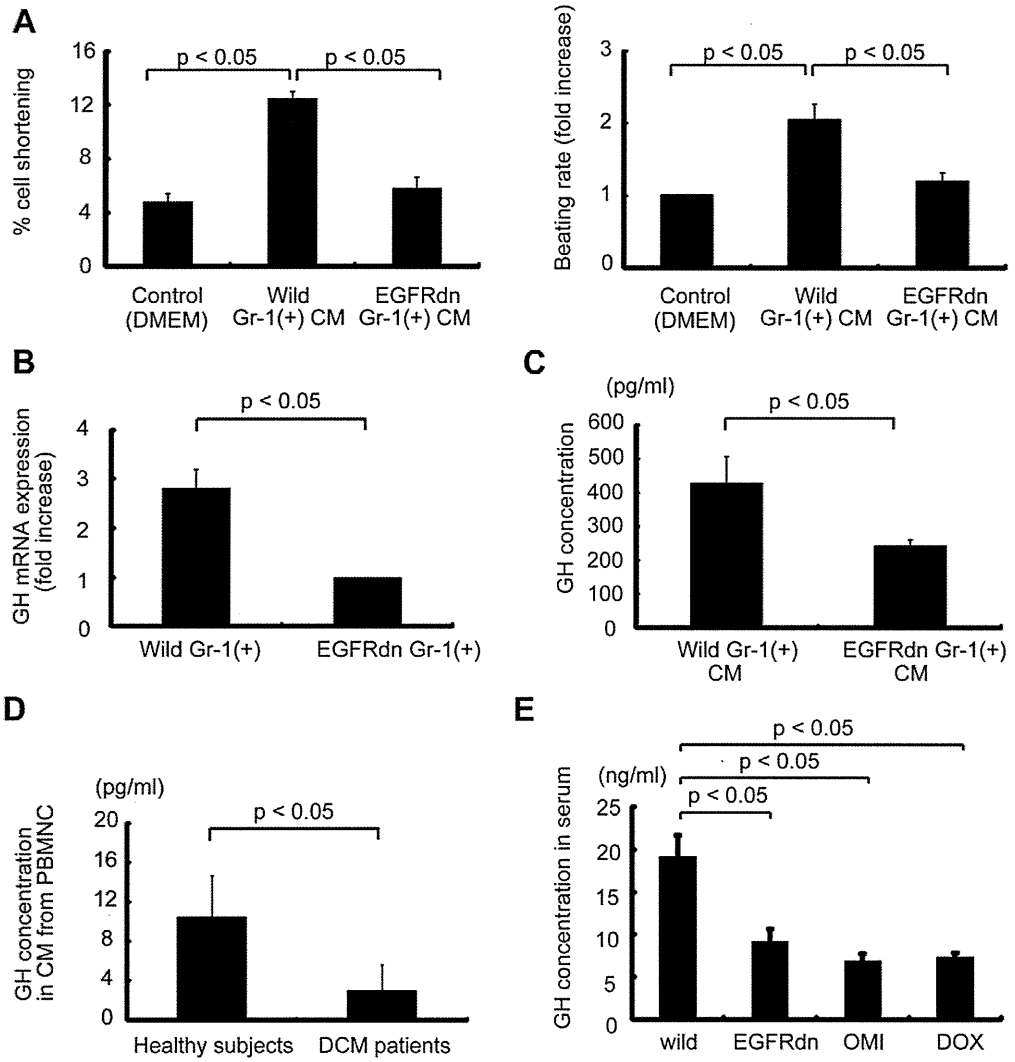

Figure 4. Analysis of secreted factors. (A) CM from Gr-1(+) cells from wild-type mice significantly improved the cell shortening and increased the beating rate in neonatal rat cardiomyocytes, as compared with CM from Gr-1(+) cells from EGFRdn mice. Left graph, cell shortening ($n = 24$ cells per group). Right graph, beating rate ($n = 24$ cells per group). (B) Quantitative RT-PCR analysis of GH mRNA in Gr-1(+) cells isolated from wild-type mice and EGFRdn mice ($n = 4$). (C, D) GH concentrations in (C) CM from Gr-1(+) cells isolated from wild-type mice and EGFRdn mice ($n = 4$) and (D) CM from PBMNC isolated from healthy ($n = 11$) and DCM subjects ($n = 10$). (E) GH concentration in serum from several mouse models of heart failure ($n = 4$). Data are means ± s.e.m.
doi:10.1371/journal.pone.0027901.g004

direct effects of GH in CM from Gr-1(+) cells on cardiomyocytes *in vivo* in transgenic mice overexpressing a dominant-negative mutant of STAT3 (STAT3dn) under the control of an αMHC promoter [13]. The Gr-1(+) cell CM-mediated improvements in cardiac function were not observed in DOX-treated STAT3dn mice (Figure S8), indicating that the CM improves cardiac function through activation of STAT3 in cardiomyocytes.

Upregulation of activin A in heart failure inhibits GH expression in Gr-1(+) cells

The expression of the GH gene has been reported to be regulated by transcription factors including pituitary transcription activator-1 (pit-1) [14], [15], and activin A has been reported to downregulate GH expression by reducing the stability of pit-1 [16]. Since activin A in the peripheral blood of heart failure patients has been reported to be upregulated compared with that in healthy controls [17], we investigated the role of activin A in the downregulation of GH in Gr-1(+) cells. Serum activin A levels were significantly higher in EGFRdn mice than in wild-type mice (Figure 6A), and were also elevated in other murine models of heart failure, including the OMI and DOX models (Figure S9). When Gr-1(+) cells were cultured with 400 pg/ml of activin A, a concentration equivalent to that in the peripheral blood of DCM mice, mRNA and protein levels of GH were significantly downregulated (Figure 6B), suggesting that activin A might be a key mediator of the reduced expression of GH in the Gr-1(+) cells of DCM mice. Furthermore, the serum activin A levels were remarkably higher in DCM patients (Table S1) than in healthy subjects (Figure 6A), while the GH levels in CM from peripheral blood mononuclear cells (PBMNC) of DCM patients was lower than that in healthy subjects (Figure 4D), suggesting that the

Table 1. DNA microarray analysis.

The fold increase	Gene symbol
4.9	Gh
4.3	Pdgfd
3.9	Figf
3.4	Tslp
3.2	Socs2
3.1	Lta
3.0	Bmp1
2.9	Il33
2.8	Ccl27a
2.7	Fgf20
2.6	Angpt1
2.5	Cxcl9
2.4	Il13
2.3	Fam3b
2.3	Il31
2.3	Gm6590
2.2	Spred1
2.2	Cmtm8
2.1	Kitl
2.1	Mif
2.1	Grem2
2.1	Il17d
2.1	Gdf10
2.0	Cxcl5

Each number indicates the fold-increase of gene expression in Gr-1(+) cells isolated from wild-type mice compared with those from EGFRdn mice.
doi:10.1371/journal.pone.0027901.t001

higher activin A levels might also inhibit GH expression in heart failure patients. A recent study showed that PBMNC are a major source of activin A in heart failure [17]. Since many humoral factors are known to contribute to the pathophysiology of heart failure [18], we examined whether humoral factors upregulated in heart failure might regulate activin A expression. Angiotensin II (AngII) (Figure 6C) and tissue necrosis factor-alpha (TNFα) (Figure S10A) increased the activin A levels in CM of PBMNC in a dose-dependent manner. Consistent with the previous reports [19], AngII and TNFα activated NFκB in the PBMNC (Figure 6D and Figure S10B) and AngII- and TNFα-induced upregulation of activin A in PBMNC were inhibited with a NFκB inhibitory peptide (Figure 6E and Figure S10C).

Inhibition of activin A in heart failure increases GH levels and improves cardiac function

To elucidate the role of activin A in EGFRdn mice, anti-activin A antibody was injected intraperitoneally for 2 weeks, with an alternate-day treatment regimen. Inhibition of activin A significantly increased GH protein levels in the CM from Gr-1(+) cells (Figure 6F). Furthermore, when neonatal rat cardiomyocytes were cultured with CM from Gr-1(+) cells isolated from anti-activin A antibody-treated EGFRdn mice, cell shortening was enhanced and the beating rate was increased significantly, as compared with CM from Gr-1(+) cells without antibody treatment (Figure 6G). Consistent with the upregulation of GH levels in Gr-1(+) cells by anti-activin A antibody treatment, the serum GH levels in EGFRdn mice were also increased (Figure 6H). Furthermore, FS and +dp/dt in EGFRdn mice treated with anti-activin A antibody were markedly improved compared with EGFRdn mice treated with isotype control (Figure 6H). Collectively, these results strongly suggest that inhibition of activin A improves cardiac function in non-ischemic DCM mice by restoring GH levels.

Discussion

Functional benefits of BMMNC infusion have been reported in human with ischemic heart diseases [2],[20]. Although we also observed the improvement of cardiac function of DCM model mice by BMMNC infusion, no engraftment of infused BMMNC was observed in the heart. At 3 d after infusion, BMMNC were only observed in the peripheral blood and spleen, but not in the heart, and very few GFP-positive cells were observed at 14 d even in the peripheral blood. This is consistent with the observations that BMMNC infusion only transiently improved cardiac function after infusion. These findings suggest that BMMNC improve cardiac function *via* humoral factors rather than *via* transdifferentiation into cardiomyocytes.

GH plays important roles in the protection of various tissues as well as the growth and development of many organs and whole body [21]. Serum GH levels have been reported to be low in patients with congestive heart failure [22]. Recent animal studies have demonstrated that GH treatment improves cardiac functions [23], [24]. The growth and protection of cardiomyocytes are regulated by various kinases such as Akt, Erk and Jak/Stat, and many studies have demonstrated that activation of Akt and Erk induces cardiac hypertrophy [25], [26] and prevents cardiomyocytes from stress-induced apoptosis [27]. Transgenic mice with cardiac-specific overexpression of the *stat3* gene were reported to show marked ventricular hypertrophy [28], while the cardioprotective effects of several cytokines including granulocyte colony-stimulating factor were reduced in mice with cardiac-specific expression of dominant-negative *stat3* [29]. In this study, we showed that GH produced by Gr-1(+) cells activated Akt, Erk, Jak2, Stat3/5 and PKA, and increased the levels of cAMP in neonatal rat cardiomyocytes (Figure 5C, D). GH has been reported to increase cAMP and activate PKA in reproductive organs by still-unknown mechanisms [30]. Here, we found that the beneficial effects of CM from Gr-1(+) cells on cardiac function were inhibited in cardiac-specific STAT3dn mice, suggesting that GH secreted by Gr-1(+) cells directly affects cardiomyocyte contractility. It has been reported that GH exerts some functions through the induction of IGF-1 expression [31], [32], and IGF-1 also promotes several cardioprotective effects in part by activating the Akt/phosphatidylinositol 3-kinase pathway [33], [34]. In the present study, the specific GH receptor inhibitor, but not anti-IGF-1 antibody, attenuated the improvements of cardiac contractility by the treatment of CM from Gr-1(+) cells in vitro (Figure 5A, B) and in vivo (Figure 5E, F). These findings suggest the effects of Gr-1(+) cells-derived CM on cardiac function of DCM mice mainly depend on GH rather than IGF-1.

It has been reported that the expression of GH gene is regulated by pit-1 at the transcriptional level [14], [15] and that activin A destabilizes pit-1 by phosphorylation [16]. Consistent with a previous report showing higher serum activin A levels in heart failure patients than in healthy controls [17], we found that serum levels of activin A were increased while GH levels in PBMNC CM were decreased in DCM patients. Similarly, the activin A levels were higher in the peripheral blood of DCM mice than in wild-type mice and activin A inhibited the production of GH in Gr-1(+)